Susceptibility weighted imaging in cerebral hypoperfusion—can we predict increased oxygen extraction fraction?

Chandrasekharan Kesavadas · Kannath Santhosh · Bejoy Thomas

Abstract

Introduction Increased concentrations of deoxyhemoglobin within veins can induce susceptibility changes resulting in increased conspicuity in susceptibility weighted imaging (SWI). Compensatory mechanisms following reduced cerebral perfusion due to carotid occlusive disease may not be sufficient to meet demands of ischemic tissue and increased tissue oxygen extraction ratio results in relative increase in deoxyhemoglobin levels in the venous blood draining affected hemisphere. We assessed whether patients with carotid disease display prominence of veins over affected cerebral hemisphere.
Methods Eighteen patients with unilateral carotid occlusion or critical carotid stenosis proven by magnetic resonance angiography (MRA) were selected. The medical records and MRI findings including SWI and MRA were reviewed. The SWI images were studied for the presence of asymmetry of veins over the cerebral hemispheres and were correlated with the site and severity of stenosis or occlusion. The veins were assumed to be conspicuous and asymmetric if there were more numerous veins and/or large veins with greater signal loss observed compared with opposite normal hemisphere.
Results In about half of patients, prominence of veins was noted in the cerebral hemisphere ipsilateral to side of occlusion. This was not observed in patients with significant extracranial carotid stenosis. The SWI abnormalities were seen extending beyond the boundaries of occluded vascular territory. There was good agreement between two observers in all the patients who showed positive finding. Also there was no interobserver variation in patients with negative findings.
Conclusion The increased susceptibility arising out of increased deoxyhemoglobin to oxyhemoglobin ratio leads to visualization of prominent veins over the affected cerebral hemisphere on SWI.

Keywords SWI · Cerebral hypoperfusion · Carotid occlusion · Cerebral veins

The first and second authors have equal contribution.

C. Kesavadas (✉) · B. Thomas
Department of Imaging Sciences and Interventional Radiology,
Sree Chitra Tirunal Institute
for Medical Sciences and Technology,
Trivandrum 695011, India
e-mail: chandkesav@yahoo.com

K. Santhosh
Department of Radiology, Sree Ramachandra Medical College,
Porur,
Chennai, India

Introduction

Hemodynamic stress induced by chronic cerebral hypoperfusion can result in various physiological adaptations to meet the demands of ischemic cerebral tissue. Hemodynamic changes resulting from progressive decline in cerebral perfusion pressure are categorized in three stages as described by Powers et al. [1, 2]. In stage 0, cerebral perfusion pressure (CPP) is normal; cerebral blood flow (CBF) closely matches with the metabolic demands of the tissue and oxygen extraction fraction (OEF) remains the same. As the degree of hemodynamic compromise increases, the cerebral arterioles dilate in response to reduced CPP, thereby increasing cerebral blood volume thus maintaining CBF (stage 1). OEF remains the same at this stage. With severe reductions of CPP, maximal autoregulation is inadequate to meet the demands, and the tissue responds to this state by increasing the OEF (stage 2). This stage of decreasing CBF with increasing OEF is termed as misery perfusion [3]. It is important to recognize

this stage because it has been shown that an increase in OEF along with reduced CBF is associated with increased risk of stroke [4]. However, these stages are not rigidly observed in physiological systems, and reductions in CBF and elevations in OEF are even observed throughout the autoregulatory phase at variable degrees [4, 5].

Though positron emission tomography (PET) has been used as gold standard for the investigation of cerebral hemodynamic variables in chronic hypoperfusion; other modalities like single photon emission computed tomography (SPECT), Xe-SPECT, CT perfusion, and MR perfusion are being evaluated. There are few studies reporting utility of MR in the assessment of cerebrovascular reactivity and hemodynamic parameters [6, 7]. All these modalities can provide quantitative or semiquantitative information regarding the hemodynamic status of a given clinical situation. PET and SPECT studies give an accurate picture of degree of hemodynamic compromise; however, they are not widely used for these studies. The variability of cerebral perfusion due to steno-occlusion can lead to false assumption of input function in the case of MR perfusion studies, and this can confound the perfusion data in many occasions. Although it was hypothesized that susceptibility weighted imaging (SWI) can be used to evaluate cerebrovascular reactivity, no major studies have been reported in this regard [8, 9].

The principles and technique of SWI have been described extensively by Haacke et al. [10]. In brief, this is a sequence that is highly susceptible to the presence of paramagnetic substances such as iron, calcium, and blood products such as deoxyhemoglobin and methemoglobin and has found its application primarily to demonstrate blood products and calcifications in various pathological conditions. The phase information of the raw MR data is initially unwrapped using homodyne demodulation method to obtain a phase mask which is then normalized and is multiplied by the original magnitude image by four times to yield images that improved the conspicuity of tissues with varying susceptibilities [11]. The utility of this sequence in various neurological diseases of children and adults has been increasingly reported [8, 12, 13].There are few anecdotal reports on the ability of SWI to demonstrate regions of increased oxygen extraction [8, 9, 12]; there are no studies described as yet in the literature addressing this issue. Though gradient echo sequences (GRE) are commonly employed to detect susceptibility effects, numerous studies have demonstrated the superiority of SWI over GRE in detection of hemorrhages and other paramagnetic substances [12]. GRE also has been correlated with increased BOLD effect due to elevated deoxyhemoglobin in acute cerebral ischemia secondary to major vascular occlusion [14]. Being a highly sensitive sequence for substances that produce susceptibility effects, SWI can also be expected to reveal such findings, probably with

improved conspicuity in similar circumstances. In this study, we intend to document the imaging findings of chronic cerebral hypoperfusion in SWI and discuss its possible pathophysiological and hemodynamic correlates. To the best of our knowledge, no such study has been described in English literature to date.

Materials and methods

The study included retrospective analysis of data from 18 patients with conventional or MR angiographically proven chronic carotid occlusion or critical carotid stenosis who were admitted to our hospital between January 2007 and November 2008. Institutional review board approval and informed consent were waived for this retrospective study. The database of hospital records were searched for key words such as "carotid artery, occlusion, stenosis", and the patient details were retrieved and were analyzed for the degree of occlusion, chronology of the disease, historical and demographic information, timing of MR imaging, and availability of necessary imaging data. Subjects were included if there was complete carotid occlusion or more than 90% stenosis of internal carotid artery confirmed either by MR or conventional angiography, and MRI including SWI were available for review. Subjects were excluded if hyperintense signal changes (DWI restriction or T2 shine through of <2 weeks duration) were observed in DWI or when images were of suboptimal quality. An age-matched control group comprising of ten patients with normal MRI brain (including SWI) and MR angiography were included for comparison. These patients had undergone MRI with MR angiography as per the advice of neurologist to rule out cerebrovascular diseases.

All the patients underwent MR imaging with a 1.5 Tesla superconducting MR system (Avanto SQ engine; Siemens, Erlangen, Germany). The MR imaging protocol included SWI sequence in addition to routine sequences such as T1, T2, FLAIR, and DWI sequences. The methodology and principles of SWI sequence is described in detail by various authors [10, 11]. In short, SWI is a high-resolution full-velocity compensated 3-D gradient echo MR sequence wherein phase images are used to create a phase mask after unwrapping and high pass filter which is then multiplied with magnitude images to enhance the conspicuity of small veins and paramagnetic substances. The imaging parameters of SWI were as follows: TR-48 ms; TE-40 ms; flip angle-20°; bandwidth-80 kHz; matrix size-512×256, slice thickness-2 mm, 56 slices in a single slab, and iPAT factor of 2. The acquisition time was 2.58 min. Post-processing was performed, and 9–12 thick minimum intensity projection (mIP) slabs were generated. Contrast enhanced MRA and/or conventional angiography of neck and intracranial arteries were also obtained in all the

patients. MRA were obtained with FLASH 3D sequence using care bolus technique with coverage from base of the neck till circle of Willis with TR-3.52 ms, TE-1.1 ms, flip angle 30°, NEX-1, bandwidth-380 kHz, base resolution 84× 80 and centric K space sampling.

The data collection and assessment of eligibility criteria were performed by a radiologist and the images of selected subjects were reviewed independently by two different neuroradiologists who were blinded to the clinical data and to each other's findings. Both the neuroradiologists were experienced in reporting SWI images since the last 3 years. The findings of the SWI images were reported before reviewing all the other sequences. After ensuring that the images obtained were of adequate quality, the SWI was studied for the presence of asymmetric intracranial cortical veins that were categorized as more numerous and/or more conspicuous in size and signal intensity in comparison to other cerebral hemisphere. Later conventional sequences were evaluated for the presence of chronic infarctions, gliotic changes as well as atrophy. FLAIR and DWI images were reviewed to assess the presence of collaterals and acute infarctions. Lastly, the angiographic findings were studied for the side of affection, location, severity and presence of collaterals. Source images of MRA were reviewed in patients with total occlusion to rule out trickle flow. These findings were correlated with the findings in SWI. Statistical analysis included Fischer exact test to assess the significance and kappa statistics to assess the interobserver variations.

Results

A total of 18 patients (15 males and three females) satisfied the inclusion criteria and were selected for the study. The mean age of the patients was 50 years (range, 22 to 83 years). Complete occlusion of either of the carotid arteries was present in 83% of the subjects and more than 90% stenosis in rest 12% of the patients. Proximal ICA was the common site of involvement (72%) followed by distal ICA (17%) and CCA (11%).There were no intracranial stenosis among the patients evaluated. CEMRA was obtained in all the patients, and DSA was additionally performed in three patients. More than half of the patients presented with clinical history of acute stroke or TIA. MRI showed hyperintense bands along the centrum semiovale, nonspecific white matter hyperintensities, and old infarcts with gliosis at the side of involvement in most of the cases. Acute infarcts were not present in any of the patients included. FLAIR sequence did not reveal the presence of any hyperintense vessels over the affected hemisphere attributed to collateral formation. Three patients had subacute infarcts; in one patient, the infarction was located contralateral to the region of occlusion and in the other

occlusion was documented earlier in the course of illness. Time of imaging from the onset of symptoms varied from 18 h to 9 months. The clinical details and imaging data are shown in Tables 1 and 2.

SWI showed more numerous veins and/ or conspicuous large veins over the side of affection in more than half of the studied subjects (ten patients). Seven patients showed no significant difference in appearance in both the cerebral hemispheres, and in one patient, the observed veins were less in the affected hemisphere. More than half of the patients (66%) with carotid occlusion showed conspicuous veins over the ipsilateral cerebral hemisphere (Figs 1 and 2). None of the patients in the stenosis group demonstrated this finding. The two venous signs (more numerous veins and/or conspicuous large veins) evaluated for in this study were observed together in most of the patients who manifested SWI abnormalities (nine of ten patients).When visualized, veins were not restricted to the arterial territories and extended beyond the vascular boundaries.

There were no alterations of the signal intensities in the dural venous sinuses. We further analyzed for the presence of any correlation between the SWI findings and infarction patterns among the patients with complete occlusion, the results of which are shown in Table 3. For this, the patients with hyperintense changes or small infarcts in the watershed zones were grouped together and were compared with large cortical infarctions. Since stenosis group did not demonstrate any SWI findings, it was not included in this analysis. All the patients with absent infarcts (three subjects) and two of three patients with small watershed infarcts demonstrated SWI findings whereas only about half of the patients (five of nine subjects) with large cortical infarcts showed positive finding. SWI findings were not correlated with collaterals in this study since MRA is not a good imaging method to demonstrate directionality of flow and detection of pial collateralization.

There was substantial interobserver agreement between the two readers in identifying the venous signs in SWI (Kappa-0.8; Table 4). None of the subjects in the control group showed asymmetry of cerebral veins over the cerebral hemispheres. Sensitivity and specificity of this finding was 55.5% and 100%, respectively. When the carotid stenosis patients were excluded from the analyses, the sensitivity increased to 66.6%. Fischer exact probability test showed that the observed finding between the test and the control group is significant (p value <0.01).

Discussion

Hemodynamic status of cerebral circulation in vivo can be indirectly assessed using many imaging techniques. Most of these derive the useful information by assessing the various

Table 1 Clinical details.

S no.	Age/sex	SWI		MRI	MRA/conventional angiography	Presentation	Timing of MR from last symptoms
		More numerous	Greater signal loss/larger veins				
1	65/M	Yes	Yes	Linear hyperintense band along left CSO and old infarct left parietooccipital region	Complete occlusion of left ICA	Acute right-side weakness	2 months
2	83/M	No	No	Hyperintensities in the left parietal and frontal lobe	90 % Occlusion of right ICA, 50 % of left ICA	Acute left-side weakness	30 days
3	39/ M	Yes	No	Left CSO hyperintensities	Complete occlusion of left CCA and ICA	TIA	42 days
4	52/M	Yes	Yes	Linear hyperintensity along the right CSO	Complete occlusion of right ICA	Acute left-side weakness	45 days
5	51/M	Yes	Yes	Linear hyperintensity along the left CSO and old infarcts in left frontal lobe	Complete occlusion of left ICA	Multiple stroke-like episode	6 months
6	60/F	No	No	Subacute infarct left basal ganglia, hyperintensities in the right basal ganglia, internal capsule	>90 % narrowing of right petrous ICA	TIA	18 h
7	39/F	Yes	Yes	Subacute infarct right corona radiata and CSO	Complete occlusion of right CCA	Multiple strokes	4 months
8	67/M	No	No	Old infarct right temporoparietal region	Complete occlusion of right ICA	Minor stroke	28 days
9	55/M	Yes	Yes	Old infarct left anterior frontal lobe	Left cavernous ICA occlusion	Ataxia and dysphagia	3 days
10	55/M	No	No	Old infarct left parietotemporal region	Complete occlusion of left ICA	Acute right-side weakness	4 months
11	61/M	Yes	Yes	Old infarct left CSO and right frontal lobe subcortical infarct	Complete occlusion of right ICA	Dysphasia	3 months
12	62/F	Yes	Yes	Hyperintense band along left CSO	Complete occlusion of left ICA	Asymptomatic	6 months
13	60/M	No	No	Small infarct left corona radiata	Complete occlusion of left ICA	TIA	9 months
14	36/M	No	No	Old infarct bilateral anterior frontal lobe	Complete occlusion of left ICA	TIA	2 months
15	57/M	More on the opposite side	No	Old infarct right temporoparietal region	Complete occlusion of right ICA	Old stroke left-side	4 months
16	22/M	No	No	Hyperintensities in the left parietooccipital lobe	>90% Narrowing of left supraclinoid ICA	Acute right-side weakness	32 days
17	54/M	Yes	Yes	Hyperintense band along both CSO, subacute infarcts watershed zones of MCA	Complete occlusion of left ICA	Subacute stroke, right side	35 days
18	29/M	Yes	Yes	Old infarct in the right insula and frontal lobe,	Complete occlusion of right ICA	Left hemiplegia	2 months

hemodynamic parameters such as CBF, CBV (cerebral blood volume), CMRO2 (cerebral metabolic rate of oxygen), and OEF. These parameters can be used to understand the perfusion status, cerebrovascular reserve, and autoregulatory mechanisms in occlusive arterial diseases. Autoregulatory mechanisms are tightly coupled with cerebral perfusion pressure (CPP).Once the CPP falls beyond a certain limit; cerebral autoregulatory mechanism compensates to meet the

Table 2 Imaging data.

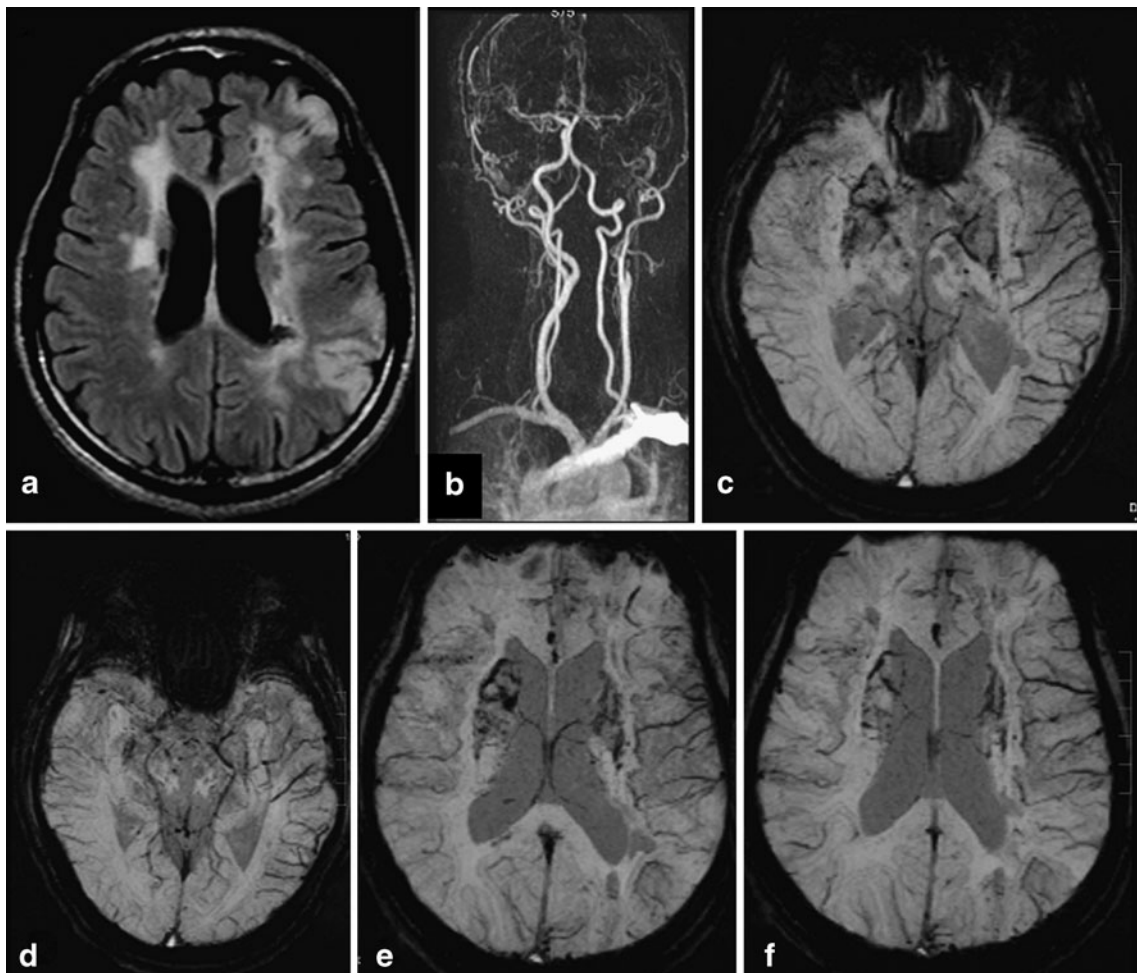| Severity of carotid stenosis	SWI appearance of veins over the cerebral hemisphere			Total
	Veins equal in both hemispheres	Prominent over the side of occlusion	Less over the side of occlusion	
Occlusion	4	10	1	15
Tight stenosis	3	…	…	3
Total	7	10	1	18

Fig. 1 a–f Case 17: FLAIR axial image (**a**) shows lacunar infarcts in bilateral centrum semiovale (CSO) and subacute infarcts in the left frontal and temporoparietal region. MRA demonstrates complete occlusion of left ICA from its origin (**b**). SWI axial images (**c** through **f**) demonstrate prominent veins over the left cerebral hemisphere. Note increased mineral deposition in both basal ganglia
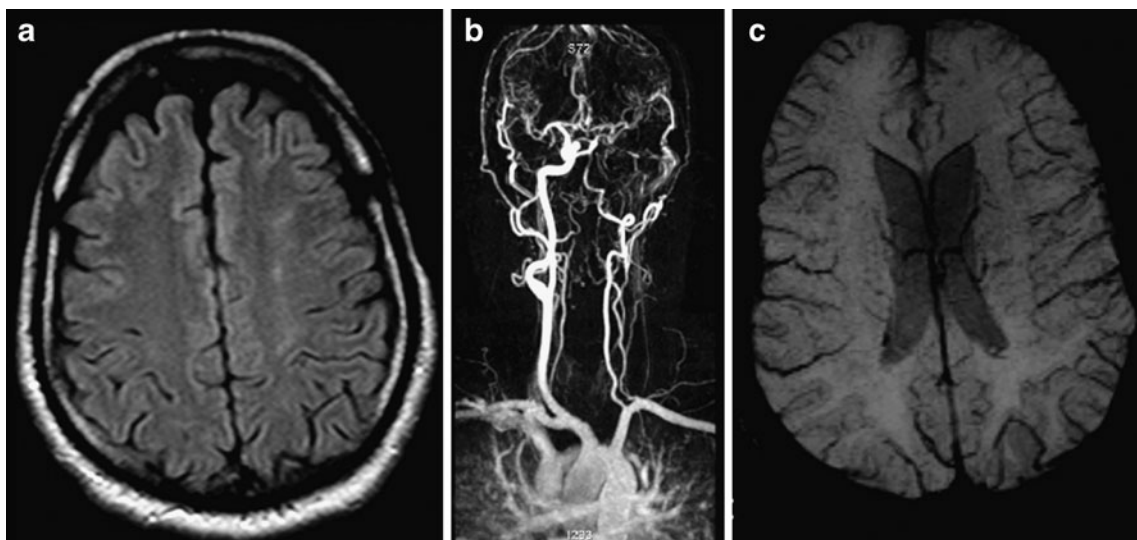

Fig. 2 a–c Case 3: Except for minimal nonspecific hyperintensity of left CSO, FLAIR axial reveals an essentially normal study (**a**). MRA reveals complete occlusion of left ICA and CCA (**b**). Prominent and increased veins over the cerebral hemisphere are clearly demonstrated in SWI (**c**)

Table 3 Correlation between the SWI findings and infarction patterns among the patients with complete occlusion.

MRI findings	SWI changes		Total
	Present	Absent	
Large cortical infarction	5	4	9
Absent infarctions/small water shed infarcts	5	1	6
Total	10	5	15

increased demand through vasodilatation and decreased vascular resistance and thus maintains CBF. Further fall in CPP results in failure of autoregulation and the CBF begins to decline. At this stage, OEF progressively increases and ensures adequate supply of oxygen to the brain tissue. More severe reduction in CPP leads to failure of all these mechanisms and results in cerebral infarction [2].

PET studies have demonstrated that the presence of increased OEF with reduced CBF in atherosclerotic carotid occlusive diseases is a recognized independent risk factor predicting future stroke in symptomatic patients [2, 15]. At present, only PET can reliably measure OEF quantitatively in tissues under stress [16]. However, PET is not widely available for clinical use, and it needs cyclotron to produce certain isotopes such as O-15 which is used to measure flow [17]. Studies with angiography showed no correlation with increased OEF in carotid occlusion [16]. Recently, role of MR imaging has also been investigated to study cerebrovascular reserve (CVR) in patients with chronic cerebral hypoperfusion. Dynamic susceptibility contrast enhanced MR was found to be inaccurate in absolute quantification of CBF when compared with PET [7]. Another method of MR that has found promising to evaluate CVR and related compensatory mechanisms is blood oxygen level dependant (BOLD) MRI.

BOLD CVR is based on the paramagnetic property of deoxyhemoglobin similar to fMRI. Deoxyhemoglobin localized within the microvascular compartment induces local magnetic heterogeneity in the adjacent diamagnetic tissue resulting in loss of signal intensity. The magnitude of signal

Table 4 Interobserver agreement.

Reader 1	Reader 2			
	More	Equal	Less	Total
More	8	0	0	8
Equal	2	7	0	9
Less	0	0	1	1
Total	10	7	1	18
Kappa=0.8				

drop is dependent on the amount of deoxyhemoglobin concentration and size of microvasculature [7]. The changes in BOLD CVR are global and are dependent on the rate of oxygen consumption of tissue, blood volume, and wash out of metabolites. Tong et al., in their review of clinical applications of SWI in children, had suggested that SWI may be able to demonstrate increased oxygen extraction in the regions of infarction or tissue hypoxemia [12]. This possibility was also suggested by others [8, 9], though, to our knowledge, no studies have been described. Recently, Morita et al. reported the presence of hypointense and enlarged vessels in GRE sequences within the acute ischemic territories due to major artery occlusion which they attributed to the BOLD effect secondary to elevated deoxyhemoglobin [5]. However, there are no reports in literature evaluating the utility and application of susceptibility imaging in chronic hypoperfusion states. BOLD effect can theoretically exist in chronic cerebral hypoperfusion due to mechanisms different from that observed in acute ischemia.

In our study, we have demonstrated the presence of asymmetric, numerous, and large vessels over the ipsilateral cerebral hemisphere in more than half of the patients with carotid occlusion. Such a finding was not observed in any of the patients with critical carotid stenosis. A clarification is needed here as to whether these vessels represented prominent veins or whether they are arterial collaterals that occur in occlusive states. These vessels were assumed to be veins based on following premises. First, as the severity of carotid occlusion increases, the CBF progressively declines and OEF increases as a compensatory mechanism to maintain the CPP. Due to maximal extraction of oxygen by ischemic tissue, deoxyhemoglobin concentration and deoxy- to oxyhemoglobin ratio increases in the draining veins [7]. This induces susceptibility effect detectable with sequences such as SWI. Indeed, the initial application of SWI was to evaluate the small intracranial veins independent of arteries [11]. The FLAIR vascular hyperintensity (FVH) sign described in carotid stenosis, occlusion, or acute infarction has been shown to correlate with collateral flow, and this is thought to be secondary to slow sluggish flow within the collaterals [18, 19]. Authors' personal experience with acute ischemia and moyamoya diseases showed that patients with exuberant collaterals had normal finding in SWI sequence (Fig. 3). Liebeskind suggested that augmented extraction of precapillary oxygen by adjacent brain tissue leads to elevation of intravascular deoxyhemoglobin with in the collaterals and this in turn could be detected by gradient MR as blooming [20]. Secondly, these vessels show no territorial preferences unlike arteries and are visualized either over the entire cerebral hemisphere or are localized to the regions collaterals are less expected.

The presence of increased veins over the affected hemisphere may have a role in evaluating patients with chronic
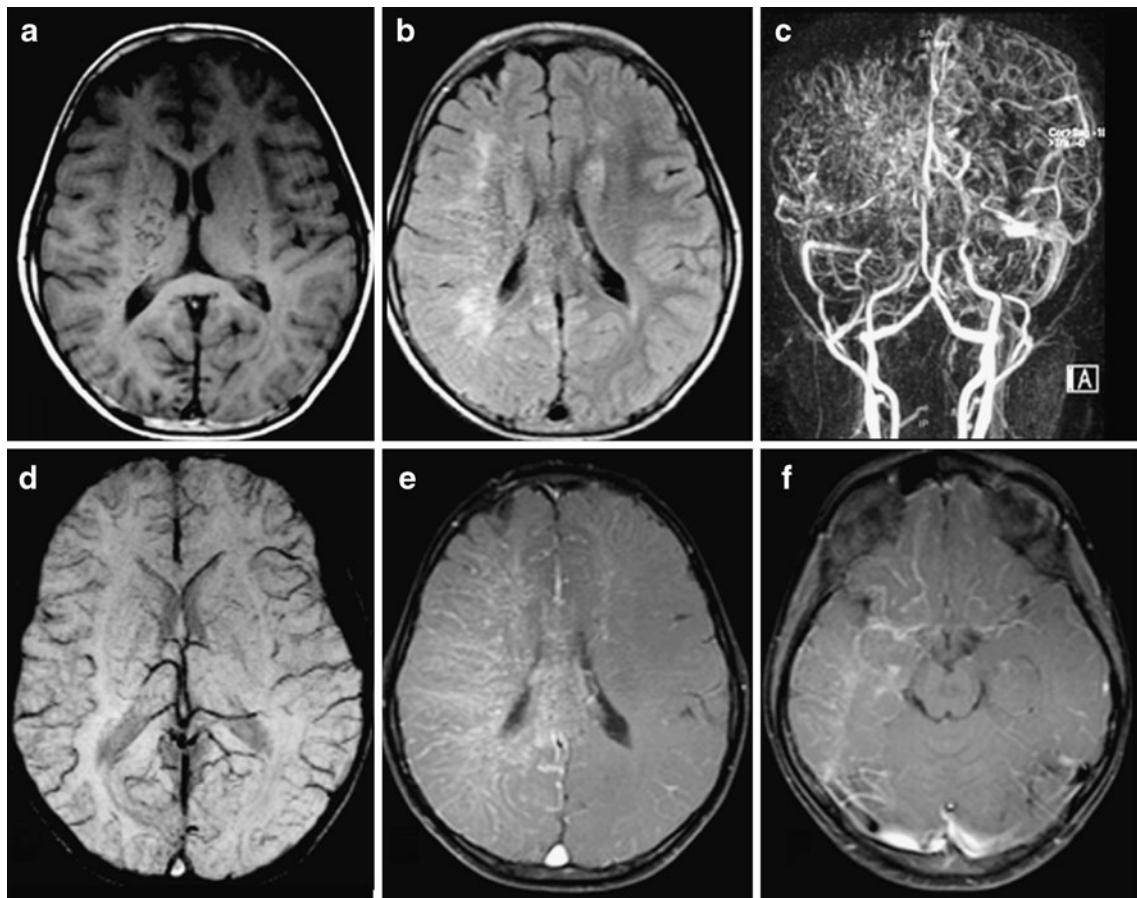
Fig. 3 Axial T1 (**a**), Axial FLAIR (**b**), contrast enhanced MRA (**c**), SWI (**d**) and contrast enhanced T1 (**e**, **f**) in a patient with bilateral supraclinoid carotid and distal basilar occlusion with moyamoya pattern and exuberant collaterals. Note the multiple collaterals in the contrast enhanced MRA and T1 images. However, the SWI images do not show prominence of blood vessels

cerebral hypoperfusion. Often, the initial evaluation of these patients includes MRI and MRA and addition of SWI sequence to the routine protocol does not prolong the examination time (SWI takes 2.5 min in 1.5T scanner) or cost much and in fact it may provide some information regarding the physiological status of the vasculature at least in a proportion of patients. The detection of prominent veins over the cerebral hemispheres may suggest an elevated deoxyhemoglobin to oxyhemoglobin ratio and reflect hemodynamic status of the vasculature. This observation was not detected in half the patients with carotid occlusion and in none of the patients with carotid stenosis. This may be due to the presence of good collateralization or compensated autoregulatory mechanisms adequate enough to maintain CPP or reduced oxygen demand in chronic infarctions. Only one patient in our series demonstrated reduced veins in the affected hemisphere. This patient had large infarct with gliosis in the right temporoparietal region and we presume, probably the latter mechanism was responsible for this observation. Among the stenosis cohort, probably the reduced but maintained flow was sufficient to keep the perfusion of capillaries and hence the CPP. There were no false positives in our study suggesting

that asymmetrical veins are not seen in normal subjects. Though the findings were subjective, the interobserver agreement was good between the two readers.

Furthermore, SWI findings were observed in majority of the patients with small watershed or absent infarcts, while only about a half of patients with large cortical infarcts demonstrated this finding in our study. The infarction occurs when the autoregulatory mechanisms and elevated OEF fails to maintain adequate perfusion, and hence, the BOLD effect is dependent on the metabolic needs of remaining surviving tissues and compensatory collateral supply. However, in patients without major infarcts, BOLD phenomena is dependent on complex interplay of autoregulation, elevation of OEF and collateralization, which, at present, can be unraveled to certain extent by PET studies. The small cohort size in this study precludes making any assumptions from this observation; hence, a larger study comparing both the cohorts is imperative.

It has been shown by Derdeyn et al. that the presence of increased OEF (misery perfusion) is associated with increased stroke in symptomatic patients [1]. The findings described in our study may have value in evaluating the

patients with chronic carotid occlusive diseases as it might suggest the presence of reduced perfusion with resultant hemodynamic variations in the affected hemisphere. Phase images of SWI have been utilized in the quantitative evaluation of iron sources in the brain in healthy and disease states with clinical and high-field MRI systems [21, 22]. Petridou et al. quantified intravascular deoxyhemoglobin and had correlated with the observed contrast difference between gray and white matter in phase images at high-field MRI [23]. Haacke et al. demonstrated a method to measure in vivo blood oxygen saturation utilizing susceptibility changes that follows a cortical activation [24]. It is unsure at the moment whether quantification of intravascular deoxyhemoglobin and hence the information regarding the perfusion and metabolic rates are possible with the current methods; however, SWI with novel mapping techniques [24] has the potential to delineate physiological changes occurring in the vascular and cellular level.

Our study has several important limitations. The aim of the study was to describe the SWI appearances in chronic cerebral hypoperfusion, and since this being a retrospective study, we could not compare our data with perfusion studies. A qualitative data analysis was performed in this study, and hence, a PET confirmation would have been ideal to confirm the findings; however, PET is not available in our institution. The findings are often subtle and require considerable experience in reporting SWI images to detect these changes. Further prospective studies with larger cohort size, correlating SWI with perfusion can help understand the pathophysiological mechanisms for variable appearances in hypoperfusion states.

Conflict of interest statement We declare that we have no conflict of interest.

References

1. Derdeyn CP, Yundt KD, Videen TO, Carpenter DA, Grubb RL Jr, Powers WJ (1998) Increased oxygen extraction fraction is associated with prior ischemic events in patients with carotid occlusion. Stroke 29:754–758
2. Grubb RL Jr, Derdeyn CP, Fritsch SM et al (1998) Importance of hemodynamic factors in the prognosis of symptomatic carotid occlusion. JAMA 280:1055–1060
3. Baron JC, Bousser MG, Rey A, Guillard A, Comar D, Castaigne P (1981) Reversal of focal "misery-perfusion syndrome" by extra-intracranial arterial bypass in hemodynamic cerebral ischemia: a case study with 15O positron emission tomography. Stroke 12:454–459
4. Derdeyn CP, Videen TO, Yundt KD et al (2002) Variability of cerebral blood volume and oxygen extraction: stages of cerebral hemodynamic impairment revisited. Brain 125:595–607

5. Schumann P, Touzani O, Young AR et al (1998) Evaluation of the ratio of cerebral blood flow to cerebral blood volume as an index of local cerebral perfusion pressure. Brain 121:1369–1379
6. Mikulis DJ, Krolczyk G, Desal H et al (2005) Preoperative and postoperative mapping of cerebrovascular reactivity in moyamoya disease by using blood oxygen level-dependent magnetic resonance imaging. J Neurosurg 103:347–355
7. Mukherjee P, Kang HC, Videen TO, McKinstry RC, Powers WJ, Derdeyn CP (2003) Measurement of cerebral blood flow in chronic carotid occlusive disease: comparison of dynamic susceptibility contrast perfusion MR imaging with positron emission tomography. Am J Neuroradiol 24:862–871
8. Santhosh K, Kesavadas C, Thomas B, Gupta AK, Thamburaj K, Kapilamoorthy TR (2009) Susceptibility weighted imaging: a new tool in magnetic resonance imaging of stroke. Clin Radiol 64:74–83
9. Hermier M, Nighoghossian N (2004) Contribution of susceptibility-weighted imaging to acute stroke assessment. Stroke 35:1989–1994
10. Haacke EM, Xu Y, Cheng YC, Reichenbach JR (2004) Susceptibility weighted imaging (SWI). Magn Reson Med 52:612–618
11. Reichenbach JR, Venkatesan R, Schillinger DJ, Kido DK, Haacke EM (1997) Small vessels in the human brain: MR venography with deoxyhemoglobin as an intrinsic contrast agent. Radiology 204:272–277
12. Tong KA, Ashwal S, Obenaus A, Nickerson JP, Kido D, Haacke EM (2008) Susceptibility-weighted MR imaging: a review of clinical applications in children. Am J Neuroradiol 29:9–17
13. Thomas B, Somasundaram S, Thamburaj K et al (2008) Clinical applications of susceptibility weighted MR imaging of the brain–a pictorial review. Neuroradiology 50:105–116
14. Morita N, Harada H, Uno M, Matsubara S, Matsuda T, Nagahiro S, Nishitani H (2008) Ischemic findings of T2*-weighted 3-Tesla MRI in acute stroke patients. Cerebrovasc Dis 26:367–375
15. Yamauchi H, Fukuyama H, Nagahama Y et al (1996) Evidence of misery perfusion and risk for recurrent stroke in major cerebral arterial occlusive diseases from PET. J Neurol Neurosurg Psychiatry 61:18–25
16. Derdeyn CP, Shaibani A, Moran CJ, Cross DT, Grubb RL, Powers WJ (1999) Lack of correlation between pattern of collateralization and misery perfusion in patients with carotid occlusion. Stroke 30:1025–1032
17. Mikulis DJ (2005) Functional cerebrovascular imaging in brain ischemia: permeability, reactivity, and functional MR imaging. Neuroimag Clin N Am 15:667–680
18. Sanossian N, Saver JL, Alger JR et al (2009) Angiography reveals that fluid-attenuated inversion recovery vascular hyperintensities are due to slow flow, not thrombus. AJNR Am J Neuroradiol 30:564–568
19. Iancu-Gontard D, Oppenheim C, Touzé E et al (2003) Evaluation of hyperintense vessels on FLAIR MRI for the diagnosis of multiple intracerebral arterial stenosis. Stroke 34:1886–1891
20. Liebeskind DS, Ances BM, Weigele JB et al (2004) Intravascular deoxygenation of leptomeningeal collaterals detected with gradient-echo MRI [abstract]. Stroke 35:266
21. McCauley G, Schrage M, Sipos P, Sun SW, Obenaus A, Neelavalli J, Haacke EM, Holshouser B, Madácsi R, Kirsch W (2010) Quantification of punctate iron sources using magnetic resonance phase. Magn Reson Med 63:106–115
22. Mittal S, Wu Z, Neelavalli J, Haacke EM (2009) Susceptibility-weighted imaging: technical aspects and clinical applications, part 2. AJNR Am J Neuroradiol 30:232–252
23. Petridou N, Wharton SJ, Lotfipour A, Gowland P, Bowtell R (2009) Investigating the effect of blood susceptibility on phase contrast in the human brain. Neuroimage 50:491–498
24. Haacke EM, Lai S, Reichenbach JR, Kuppusamy K, Hoogenraad FGC, Takeichi H, Lin W (1997) In vivo measurement of blood oxygen saturation using magnetic resonance imaging: a direct validation of the blood oxygen level-dependent concept in functional brain imaging. Hum Brain Mapp 5:341–346